Optimization of the Performance of Small Speaker Systems with Passive Radiators

Nielsen, Daniel Gert; Lee, Gyeong-Tae ; Park, Yong-Hwa; Jensen, Jakob Søndergaard; Agerkvist, Finn T.

Published in:
Proceedings of 49th International Congress and Exposition on Noise Control Engineering

Publication date:
2021

Document Version
Publisher's PDF, also known as Version of record

Seoul inter-noise 2020 23-26 AUGUST

Optimization of the Performance of Small Speaker Systems with Passive Radiators

Daniel Gert Nielsen[1]
Acoustic Technology, Department of Electrical Engineering, Technical University of Denmark
Ørsteds Plads 352, 2800 Kgs. Lyngby, Denmark

Gyeong-Tae Lee
Department of Mechanical Engineering, KAIST
291 Daehak-ro, Yuseong-gu, Daejeon 34141, Korea

Yong-Hwa Park
Department of Mechanical Engineering, KAIST
291 Daehak-ro, Yuseong-gu, Daejeon 34141, Korea

Jakob Søndergaard Jensen
Centre for Acoustic-Mechanical Micro Systems, Technical University of Denmark
Nils Koppels Allé, Bygning 404, 2800 Kgs. Lyngby, Denmark

Finn Thomas Agerkvist
Acoustic Technology, Department of Electrical Engineering, Technical University of Denmark
Ørsteds Plads 352, 2800 Kgs. Lyngby, Denmark

ABSTRACT

Small transportable Bluetooth- and smart/AI speakers are becoming an increasing part of many households. Due to their small size, these speakers have limited output at low frequencies, and typically have a vented port or in some cases a passive radiator to improve the low-frequency performance. In this work, we show how a density based material optimization approach can be used to optimize the frequency response of the system. The passive radiator is placed at the top of a cylinder with a down-firing speaker, driven with a voltage source, which, via a lumped model, is connected to a multi-physics finite element framework. The speaker radiates sound into an unbounded domain, which is realized by using perfectly matched layers. The performance of the speaker is based on a numerical measurement 1 meter away from the speaker. Several optimization results are shown and these are compared with a more generic type of small speaker system.

1. INTRODUCTION

Small compact speakers that can be controlled with voice commands are increasingly becoming a part of many households. Twenty-four percent of Americans owns at least one smartspeaker according

[1]dgniel@elektro.dtu.dk

to a recent report published by Edison Research and NPR [1]. Out of the 60 million Americans owning a smartspeaker 23 % of them use the smartspeaker for the majority of their music listening, a number which increases every year. The quality of the sound of these type of products are therefore increasingly important. The physical size and the limited cabinet space available mean that the reproduction of low frequency content can be lackluster. Presently, there are options available to extend the frequency range of speaker systems, e.g. an EQ that is targeted towards low frequencies can to some extend improve the output, this can lead to distortion if the input voltage is too high, also an overall higher power consumption is to be expected. Other popular options are vented ports or passive radiators. The passive radiator requires less space and does not produce a whistling sound which the vented port systems occasionally are prone to do.

The passive radiator was invented and patented by H. F. Olson in 1934 [2], it was, however, first in 1954 when Olson et. al. published a paper describing the design process of cabinets with 8, 10 and 12 inch loudspeakers where a passive radiator was included in the cabinet [3], that his original idea gained attention. The reason for this being, according to R. H. Small, that the design process was until then not very well described within the literature [4]. In reference [5] R.H. Small gives an in depth description of how a direct-radiator loudspeaker can be designed including a port or passive radiator.

Numerical modelling of vibro-acoustic problems are quite common these days, even complex models of loudspeakers and hearing aids can be modelled with numerical models such as Finite Element (FE) or Boundary Element (BE) models. Within the recent years many advances have been made in applying optimization techniques to improve existing designs or come up with new designs. Topology optimization has been successfully applied to acoustic-structure interaction problems [6, 7] and to the design of acoustic horns [8]. In the recent years generalized shape optimization has also been applied to vibro-acoustic problems [9]. Dilgen et al. compares the aforementioned methods in reference [10]. In reference [11] Bezolla uses parameter-, topology- and shape optimization to improve acoustic elements such as phase plugs in loudspeakers. Recently Nielsen et al. used material optimization to maximize the pressure output from a flat panel loudspeaker [12].

This paper deals with the design of a passive radiator for a small cylindrical speaker. We are utilizing FE modeling combined with a lumped parameter model (LPM) [13] and gradient based optimization techniques. The combination of these methods yields a strong tool for tailoring the frequency response of e.g. a smartspeaker. Subsequent sections will elaborate on the theory required to perform the numerical calculations, then we present the optimization scheme and finally we present and discuss the optimization results.

2. THEORY

This section will describe the model of the smartspeaker used in this paper, along with the FE and optimization theory that is used. The speaker used in this work is inspired from the Amazon Echo speaker configuration, with a down-firing woofer and tweeter. Our model is shown in Figure 1, here we have only included the woofer, since we are only interested in the low frequency output of the speaker. The figure also shows that a passive radiator is placed in the top of the speaker. The figure shows the speaker in 2D with a vertical z-axis and a horizontal r-axis, this implies that the modeling of the speaker utilizes 2D axisymmetry. In this work the woofer is excited with an electrical signal, which is included in the FE model as a lumped addition, this method and the theory required to implement it is thoroughly discussed in reference [13]. The cabinet of the smartspeaker and the acoustic lens is considered rigid.

The speaker system in Figure 1 is shown as a model problem in Figure 2. The smartspeaker is placed in an unbounded domain, here modeled with perfectly matched layers (PMLs) in the domain Ω_A, the rest of the acoustic domain is denoted Ω_a, the structural domains are denoted Ω_s, the interfaces between solid and acoustic domains are called Γ_{as} and finally Γ_a denotes the outer boundaries. The red square pinpoints the listening position 1 meter away from the smartspeaker system. The size of

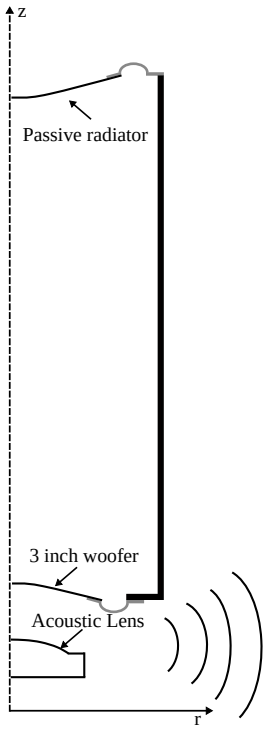

Figure 1: 2D sketch of a cylindrical smartspeaker with a passive radiator

the red square is chosen to be 5x5cm. In this area the preferred objective function is evaluated as a qualitative measure of the speakers performance.

The notation in this paper obeys the following rules; capital bold letters specifies a matrix, small bold letters implies a vector and non bold letters are scalars.

2.1. Finite Element Model

The governing equations for the time-harmonic motion of a linear elastic body where body forces has been neglected are

$$-\rho\omega^2\mathbf{u} - \nabla\cdot\boldsymbol{\sigma}(\mathbf{u}) = 0 \qquad \text{in} \quad \Omega_s \tag{1}$$

$$\boldsymbol{\sigma} = \mathbf{C}\boldsymbol{\epsilon} \tag{2}$$

$$\epsilon = \{\epsilon_r\ \epsilon_\theta\ \epsilon_z\ \gamma_{zr}\}^T \qquad \text{(2D Axisymmetric)} \tag{3}$$

$$\epsilon_r = \frac{\partial u_r}{\partial r},\ \epsilon_\theta = \frac{u_r}{r},\ \epsilon_z = \frac{\partial u_z}{\partial z},\ \gamma_{zr} = \left(\frac{\partial u_r}{\partial z} + \frac{\partial u_z}{\partial r}\right), \tag{4}$$

here ρ is the mass density of the material, ω is the excitation frequency in radians, $\mathbf{u}$ is the structural displacements, $\boldsymbol{\sigma}$ is the stress tensor, Ω_s is the structural domain, $\mathbf{C}$ is the constitutive matrix for an axisymmetric structure, $\boldsymbol{\epsilon}$ is the strain tensor, u_r is the structural displacement in the r-direction and u_z is the displacement in the z-direction.

To obtain the pressure distribution in the acoustic domain, the Helmholtz equation is solved

$$\Delta p + \frac{\omega^2}{c^2}p = 0, \tag{5}$$

here Δ is the Laplace operator in cylindrical coordinates, p is the pressure and c is the speed of sound in air. A modified Helmholtz equation [14, 15] is solved in a truncated PML region (Ω_A), as shown in Figure 2.

$$\frac{1}{\gamma_r}\frac{\partial}{\partial r}\left(\frac{1}{\gamma_r}\frac{\partial p_A}{\partial r}\right) + \frac{1}{\gamma_z}\frac{\partial}{\partial z}\left(\frac{1}{\gamma_z}\frac{\partial p_A}{\partial z}\right) + k^2 p_A = 0, \tag{6}$$

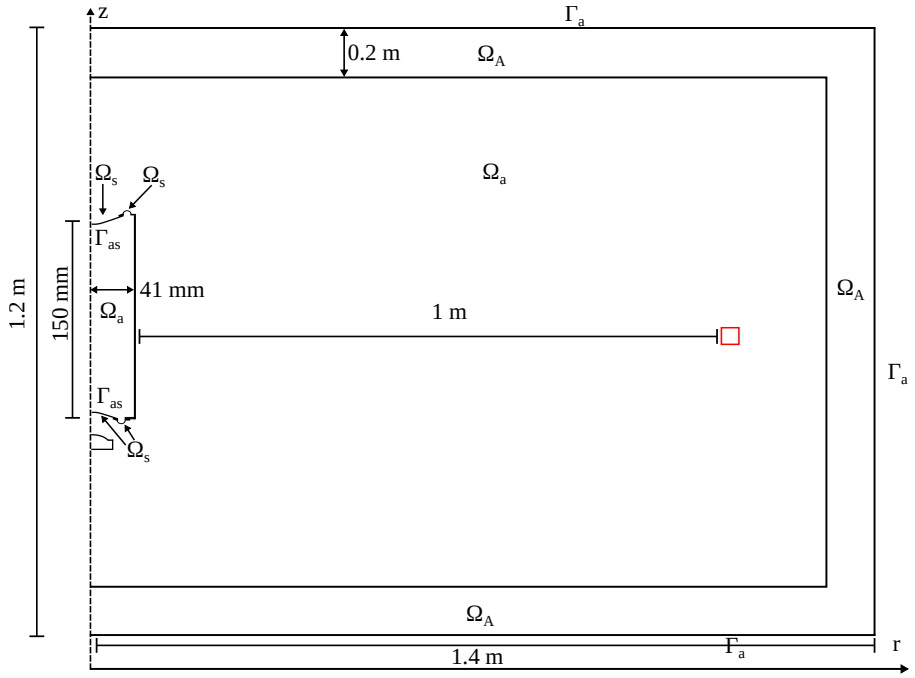

Figure 2: Sketch of the problem to be solved, with definitions of the different domains, interfaces and boundaries.

where p_A is the pressure in the PML region, the formulation of γ is from [16], here extended to accommodate for a PML in both the r- and z direction

$$\gamma_r(r) = 1 - j\kappa\left(\frac{r - r^*}{t}\right)^2 \tag{7}$$

$$\gamma_z(z) = 1 - j\kappa\left(\frac{z - z^*}{t}\right)^2. \tag{8}$$

Where r^* and z^*, indicate the interface coordinate between the PML/acoustic domain and r and z are the position within the PML, κ is the absorption coefficient with a constant value of 10 and t is half the thickness of the PML which equals 0.1m.

Equation 1 and Equation 5 are to be solved using the FE method. The FE matrices for the elastic body in Equation 1 are

$$\mathbf{K} = \int_{\Omega_s}\int_{-\pi}^{\pi} \mathbf{B}^T\mathbf{C}\mathbf{B}r \, \mathrm{d}\Omega_s \ , \ \mathbf{M} = \int_{\Omega_s}\int_{-\pi}^{\pi} \rho\mathbf{N}^T\mathbf{N}r \, \mathrm{d}\Omega_s. \tag{9}$$

Here $\mathbf{B}$ is the strain-displacement matrix, r is the radial distance to the Gauss point from the center axis z, and $\mathbf{N}$ is a matrix consisting of the quadratic iso-parametric shape functions. Damping in the mechanical components are considered as an isotropic structural loss factor, denoted η, such that $\mathbf{K} = \mathbf{K}(1 + j\eta)$, where j is the imaginary number, η equals 0.45 in the rubber surround and 0.2 in the diaphragm.

The FE matrices required to solve the Helmholtz equation in Equation 5 and the modified Helmholtz equation in Equation 6 are

$$\mathbf{K}_a = \int_{\Omega_a}\int_{-\pi}^{\pi} \left(\mathbf{N}_{a,r}^T\mathbf{N}_{a,r} + \mathbf{N}_{a,z}^T\mathbf{N}_{a,z}\right) r \, \mathrm{d}\Omega_a + \int_{\Omega_A}\int_{-\pi}^{\pi} \left(\frac{\gamma_z}{\gamma_r}\mathbf{N}_{a,r}^T\mathbf{N}_{a,r} + \frac{\gamma_r}{\gamma_z}\mathbf{N}_{a,z}^T\mathbf{N}_{a,z}\right) r \, \mathrm{d}\Omega_A \tag{10}$$

$$\mathbf{M}_a = \int_{\Omega_a}\int_{-\pi}^{\pi} \frac{1}{c^2}\mathbf{N}_a^T\mathbf{N}_a r \, \mathrm{d}\Omega_a + \int_{\Omega_A}\int_{-\pi}^{\pi} \frac{1}{c^2}\gamma_r\gamma_z\mathbf{N}_a^T\mathbf{N}_a r \, \mathrm{d}\Omega_A, \tag{11}$$

where subscript r and z refers, respectively, to the differential operator with respect to global r- and z-coordinates, $\mathbf{N}_a$ is a row vector consisting of the quadratic acoustic shape functions.

At the interface between the mechanical structure and the acoustic domain a coupling matrix, $\mathbf{S}$, is defined such that the structure acts as an acoustic source and the back induced pressure from the air acts as a surface load on the structure

$$\mathbf{S} = \int_{\Gamma_{as}} \int_{-\pi}^{\pi} \mathbf{N}^T \mathbf{n}_a \mathbf{N}_a r \, \mathrm{d}\Gamma_{as}. \tag{12}$$

Here $\mathbf{n}_a$ is the normal vector of the interface between the acoustic and structural boundary pointing outwards from the acoustic boundary.

The entire system of equations then becomes

$$\left(\begin{bmatrix} \mathbf{K} & -\mathbf{S}^T \\ \mathbf{0} & \mathbf{K}_a \end{bmatrix} - \omega^2 \begin{bmatrix} \mathbf{M} & \mathbf{0} \\ \rho\mathbf{S} & \mathbf{M}_a \end{bmatrix} \right) \begin{Bmatrix} \mathbf{u} \\ \mathbf{p} \end{Bmatrix} = \begin{Bmatrix} \mathbf{f} \\ \mathbf{0} \end{Bmatrix}. \tag{13}$$

The above equation are the standard way of solving acoustic-structure interaction problems. However, since we are dealing with loudspeakers the excitation should come from the electric motor system, which is driven with an AC voltage source. Reference [13] suggest an approach in which the electric motor system and parts of the mechanical system is lumped. This lumped system can be added to the FE system of equations in Equation 13 by adding only one equation. As shown in [13] the system of equations can be written as

$$\left(\tilde{\mathbf{K}} + j\omega\tilde{\mathbf{C}} - \omega^2 \tilde{\mathbf{M}} \right) \begin{Bmatrix} \mathbf{u} \\ \mathbf{p} \\ i_c \end{Bmatrix} = \begin{Bmatrix} \mathbf{0} \\ \mathbf{0} \\ e_g \end{Bmatrix}. \tag{14}$$

Here $\tilde{\mathbf{C}}$ is the matrix including the velocity proportional terms from the lumped model, i_c is the current in the electric motor system and e_g is applied AC voltage.

Equation 14 is for the duration of this paper written with compact notation as

$$\tilde{\mathbf{S}}\tilde{\mathbf{u}} = \tilde{\mathbf{f}}, \tag{15}$$

2.2. Optimization

We are interested in enhancing the low frequency performance of the smartspeaker in Figure 1. To do this we need to establish a measure of the output of the speaker system, an example could be the pressure squared in a listening area 1m away from the speaker. This can be described in an objective function such as

$$\phi = \tilde{\mathbf{u}}^{\mathbf{T}} \mathbf{L} \bar{\tilde{\mathbf{u}}}, \tag{16}$$

where $\mathbf{L}$ is used to select the pressure degrees of freedom (DOF) related to the 5x5cm boxed region 1m away from the speaker as shown in Figure 2 and $\bar{(\,)}$ is the complex conjugate. The objective function in Equation 16 is beneficial if we purely want to maximize the pressure squared, however, a flat response is more desirable. We therefore propose the following objective function

$$\Phi_0 = \left(Z_D - \tilde{\mathbf{u}}^{\mathbf{T}} \mathbf{L} \bar{\tilde{\mathbf{u}}} \right)^2 \tag{17}$$

here, Z_D is a target value based on the flat output above the fundamental frequency of the woofer. If the difference in Equation 17 is minimized we will obtain a flat response in the desired frequency range. The frequency range will be constructed by specifying a number of discrete frequencies, the objective function, which bears resemblance to a Chebyshev alignment, in Equation 17 is then evaluated for each frequency. This can be cast as a min-max optimization problem, here the optimizer

seeks to minimize the objective function for the discrete frequency with the largest value computed by Equation 17. The optimizer is allowed to change only the material parameters of the passive radiator. The optimization should therefore be able to control stiffness, mass and damping of the passive radiator. The above requirements leads to the following min-max optimization problem

$$\begin{array}{lll} \min\limits_{\mathbf{x}} \quad \max & \Phi_0 = \left(Z_D - \tilde{\mathbf{u}}_k^T \mathbf{L} \tilde{\tilde{\mathbf{u}}}_k\right)^2 , & k = 1, \ldots, p \\ \text{s.t.} & \tilde{\mathbf{S}} \tilde{\mathbf{u}}_k - \tilde{\mathbf{f}} = 0 , & k = 1, \ldots, p \\ & 0 \leq \mathbf{x}_j \leq 1 , & j = 1, \ldots, n \end{array} \tag{18}$$

where p is the number of frequencies, $\mathbf{x}_j$ is the design variables and n is the number of design variables. There are 20 logarithmic spaced frequencies between 90Hz and 170Hz. It is necessary to specify a fine frequency resolution, otherwise the optimizer could exploit the gap between the frequency bins and place unwanted resonances there. The above min-max optimization problem is in practice solved by using a bound formulation and imposing an extra constraints on the problem as shown below

$$\begin{array}{lll} \min\limits_{\mathbf{x},z} & z , & z \geq 0 \\ \text{s.t.} & \tilde{\mathbf{S}} \tilde{\mathbf{u}}_k - \tilde{\mathbf{f}} = 0 , & k = 1, \ldots, p \\ & \left(Z_D - \tilde{\mathbf{u}}_k^T \mathbf{L} \tilde{\tilde{\mathbf{u}}}_k\right)^2 - z \leq 0 , & k = 1, \ldots, p \\ & 0 \leq \mathbf{x}_j \leq 1 , & j = 1, \ldots, n \end{array} \tag{19}$$

In the above equations $\mathbf{x}_j$ includes the design variables α, β and ζ, which controls stiffness, mass and damping, respectively. A change in the design variable applies to the whole region to which it is assigned, e.g. if α is assigned to the diaphragm and it increases, the entire stiffness of the diaphragm is increased uniformly. The actual physical stiffness, mass and damping is determined from the design variable with a simple linear interpolation which enforces an upper and lower bound on the physical values

$$\begin{aligned} E &= E_{min} + \alpha \left(E_{max} - E_{min}\right) \\ \rho &= \rho_{min} + \beta \left(\rho_{max} - \rho_{min}\right) \\ \eta &= \eta_{min} + \zeta \left(\eta_{max} - \eta_{min}\right) . \end{aligned} \tag{20}$$

Here E is the Young's Modulus, ρ is the density, η is the structural loss factor, the subscript "min" refers to the lower bound and "max" refers to the upper bound. The purpose of the bounds are to avoid completely unrealistic material properties.

The design sensitivities are calculated with the adjoint approach which yields a semi-analytical expression for the gradients of Equation 17

$$\mathbf{S}^T \boldsymbol{\lambda} = -\left(\frac{\partial \Phi_0}{\partial \mathbf{u}_r} - i \frac{\partial \Phi_0}{\partial \mathbf{u}_i}\right)^T = 4 \left(Z_D - \tilde{\mathbf{u}}^{\mathbf{T}} \mathbf{L} \tilde{\tilde{\mathbf{u}}}\right) \mathbf{L} \tilde{\tilde{\mathbf{u}}}, \tag{21}$$

where $\boldsymbol{\lambda}$ is the Lagrange multipliers, subscripts r and i refers to real and imaginary parts of the solution vector, respectively.

The design sensitivities can then be computed as

$$\frac{d\Phi_0}{dx} = \mathrm{Re}\left(\boldsymbol{\lambda}^T \frac{\partial \mathbf{S}}{\partial x} \tilde{\mathbf{u}}\right).$$

The design sensitivities are used in the method of moving asymptotes (MMA) algorithm [17].

Table 1: Material properties for the woofer and initially also the passive radiator

	E [Pa]	ρ [kg/m^3]	η [−]	ν [−]
Diaphragm	10^{10}	1650	0.2	0.3
Surround	$40 \cdot 10^5$	1400	0.25	0.45

Table 2: Lumped parameters used to model the electric motor system, voice coil and spider.

M [kg]	L_E [mH]	n [−]	C_z [m/N]	C_r [m/N]	R [N · s/m]	Bl [T · m]	R_E [Ω]
0.0015	0.05	0.7	$1.0{\cdot}10^{-3}$	$5{\cdot}10^{-5}$	0.75	3.43	3.52

3. RESULTS

This section includes the optimization results for the tuning of the passive radiator. We are considering two cases, one case will only consider tuning the mass of the diaphragm and the damping of the surround, this example will be referred to as "mass tuned". This mimics the traditional lumped approach where one can tune the resonance of the passive radiator, as long as the suspensions is sufficiently compliant, by tuning the mass of the diaphragm. The other approach will allow stiffness, mass and damping to vary independently in the diaphragm and the surround of the passive radiator. This approach has 6 design variables and will be referred to as the 6 variable design.

Table 1 shows the material properties that are used as a starting guess for the optimization, the active loudspeaker also has these material properties. The values are typical values for a paper cone and a rubber surround.

Table 2 shows the values that are used in the LPM to model the 3 inch woofer used in this work. In the table M is the moving mass of the lumped mechanical components, L_E is the voice coil inductance, n is the fractional order derivative used to model the lossy inductor, C_z is the compliance in the z-direction, C_r is the compliance in the r-direction, R is mechanical damping, Bl is the force factor and R_E is the DC resistance in the voice coil wire. The speaker is excited by applying an AC voltage source, e_g, to the lumped circuit. In this work we apply a voltage of 1V.

The material properties of the diaphragm and surround of the passive radiator is determined by an interpolation function which is based on the continuous update of the associated design variable, as shown in Equation 20. These interpolation functions are constrained by a lower and upper bound. The values of these bounds are shown in Table 3.

Figure 3 shows the iteration history of the mass tuned example. The objective function in Figure 3a are normalized with the value of the objective function for the initial guess and it reaches a value of 0.15 after 83 iterations. Figure 3b shows the progression of the two design variables, the starting guess for the optimization is using design variable values such that the material properties corresponds to the values in Table 1. The design variables are only allowed to change 0.01 at each iteration step. Generally we see that that the optimizer increases the mass and lowers the damping. The resulting density and damping can be seen in Table 4a and the frequency response of the optimized smartspeaker are shown in Figure 5

Figure 4 displays the iteration history of the optimization with 6 design variables. In Figure 4a

Table 3: Bounds on the physical values

	E_{min} [Pa]	E_{max} [Pa]	ρ_{min} [kg/m^3]	ρ_{max} [kg/m^3]	η_{min} [−]	η_{max} [−]
Diaphragm	10^8	$40 \cdot 10^9$	1000	4500	0.05	0.9
Surround	$40 \cdot 10^3$	$16 \cdot 10^6$	1000	4500	0.05	0.9

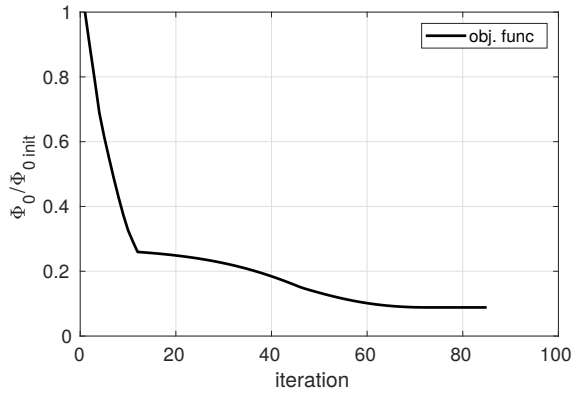

(a) Objective function

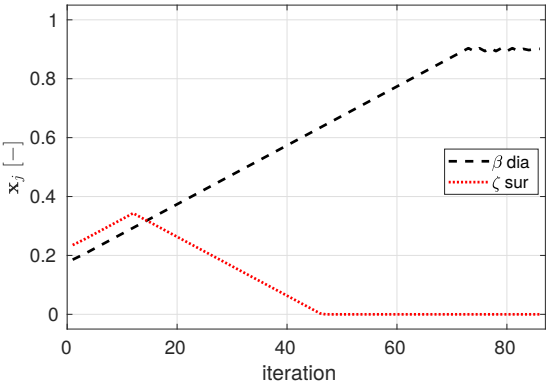

(b) Design variables

Figure 3: Mass case: (a) shows the iteration history of the normalized objective function, (b) shows the design history, here, the black curve relate to the design variable in the diaphragm and the red curve is associated with the surround

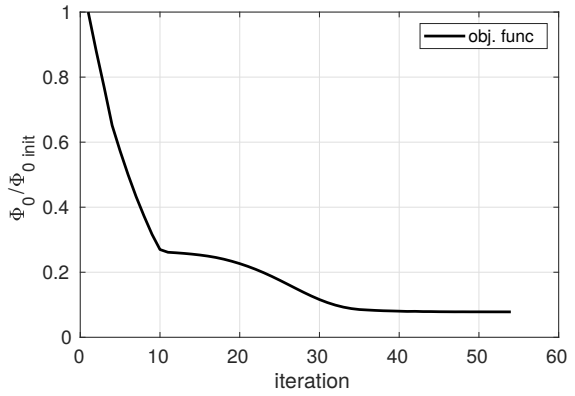

(a) Objective function

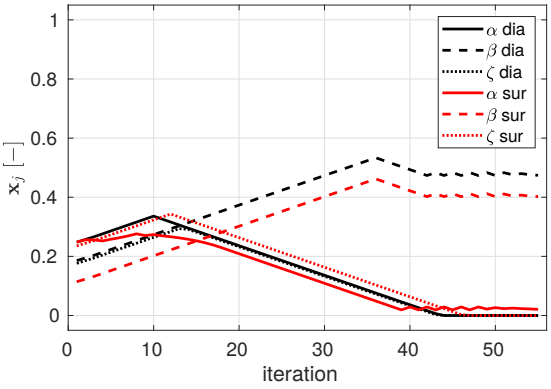

(b) Design Variables

Figure 4: 6 variable case: (a) shows the iteration history of the normalized objective function, (b) shows the design history, here, the black curves relates to the design variables in the diaphragm and the red curves are associated with the surround

one can observe that the pattern of the objective function is similar to that of Figure 3a, however, it uses fewer iterations to converge, here we reach a value of 0.13 after 61 iterations. This configuration of material parameters are therefore slightly better than the previous example. Figure 4b shows the design history. The configuration of stiffness, mass and damping is displaying differences when compared to the configuration in Figure 3b. In Figure 4b we see an increase in mass, as we expect, but the final configuration consists of a lower mass than the mass tuned example. This is due to the fact that the optimizer lowers the stiffness of the surround as the mass increases, it is therefore not necessary to increase the mass of the diaphragm as much as seen in Figure 3b. The material properties for optimized passive radiator are shown in Table 4b, the optimizer finds a material configuration that suggests that the cone of the passive radiator in this example could be made out of aluminum.

The dashed blue line in Figure 5 is the frequency response for the mass tuned passive radiator in Table 4a. This result shows that the optimizer tunes the resonance of the passive radiator such that it is lower and thereby the frequency range of the speaker system is extended. The result is a significant improvement of the output in the targeted range compared with the initial guess. Outside of the frequency range of interest we can see that towards higher frequencies the frequency response is similar to the initial guess, however, towards lower frequencies we see a very steep roll-off and a

Table 4: Material properties obtained with optimization, (a) is the results in Figure 3 and (b) is the results from Figure 4

	ρ [kg/m^3]	η [−]
Diaphragm	4155	-
Surround	-	0.05

(a) Mass and damping

	E [Pa]	ρ [kg/m^3]	η [−]
Diaphragm	10^8	2660	0.05
Surround	$37.2 \cdot 10^4$	2408	0.05

(b) All 6 variables

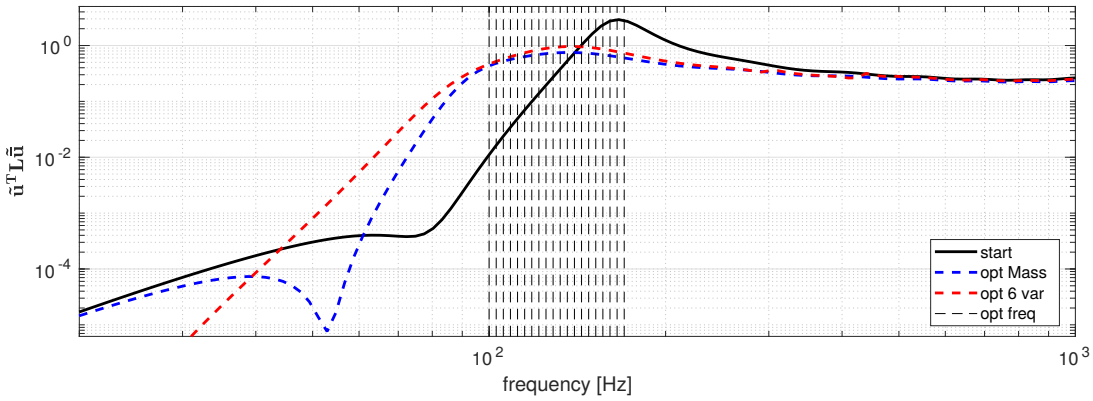

Figure 5: Frequency response function for the initial guess (solid black line), mass tuned passive radiator (dashed blue line) and the 6 variable optimization (dashed red line). The dashed vertical lines indicates the 20 logarithmic spaced discrete frequencies between 90-170Hz.

dip which can be attributed to destructive interference.

The dashed red line in Figure 5 displays the frequency response for the passive radiator for which the optimizer was allowed to tune stiffness, mass and damping in both the diaphragm and the surround. We showed earlier that the optimizer found an optimal solution where the mass was increased and stiffness and damping was decreased. This yields an almost flat line in the entire frequency range of interest, the resonance is not very prominent and the roll-of is not as steep as compared to the dashed blue line. This approach slightly improves the performance of the passive radiator compared to the mass tuned example and yields a 1 dB increase in output in nearly the entire frequency range of interest. We also see a much softer roll-of which means that the output below the frequency range of interest is enhanced compared to both the initial guess but also the dashed blue line. This comes to show that although the tuning of the mass of the diaphragm is important it does not necessarily guarantee the best result, the stiffness of the surround can have a major impact on the low frequency performance of the passive radiator. We show that if the relationship between the stiffness of the surround and the stiffness of the air inside the cabinet is tuned correctly there is more output from the passive radiator to be gained. The trade-off is that the output below 44 Hz is below both the initial guess and the mass tuned passive radiator, however, the reduction at the lowest frequencies is most likely not perceivable when listening.

Figure 6 shows the volume velocity at the surface of the passive radiator for the initial speaker system, the mass tuned system and the system with 6 design variables. From the figure the resonance frequency of the passive radiator can be estimated, the mass tuned example has a resonance frequency of 92 Hz and for the 6 variable case the resonance is 89 Hz. Notice that both the shape and size of the two curves related to the optimized examples are closely related in the frequency range specified in the optimization problem. This explains the similarity in the frequency response seen in Figure 5. The 6 variable optimization has more parameters to tune and the optimizer finds it beneficial to increase the mass and lower the stiffness in a proportional way such that the resonance frequency is

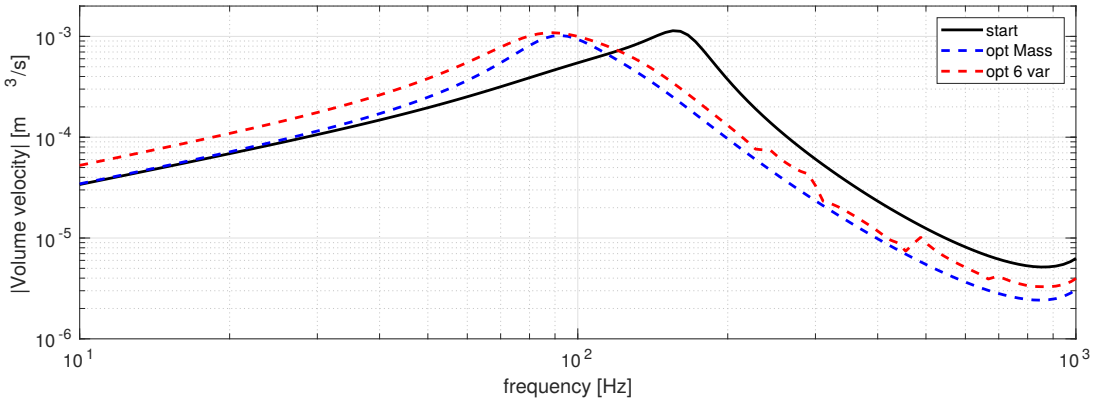

Figure 6: Volume velocity in the z-direction at the surface of the passive radiator for the initial guess (solid black line), mass tuned passive radiator (dashed blue line) and the 6 variable optimization (dashed red line)

situated close to that of the mass tuned example. This leads to an increase in the volume velocity below the resonance peak, as this is attributed to the decrease in the stiffness of the surround. The slight decrease in volume velocity above the fundamental frequency can be attributed to the increase in the mass of the diaphragm and surround. It seems that the 6 variable case is able to tune the passive resonance to be broader, i.e. similar damping but lower Q factor, which giver the system output a bit more at low frequencies.

The the dashed blue line follows the black curve below the resonance which is to be expected since the stiffness here is unchanged. Furthermore we see that the volume velocity above the resonance is the lowest compared to the two other curves due to the fact that the mass tuned example has the highest density of the diaphragm.

There are a few spikes in the volume velocity after the fundamental frequency for the 6 variable optimization case. This is due to the overall decrease in stiffness and damping for the surround and diaphragm, these spikes arise from breakup modes in the surround and diaphragm, the output from these spikes in volume velocity are however barely noticeable in the pressure response in Figure 5.

4. DISCUSSION

In this work we use min-max optimization to formulate an optimization problem to be solved. The formulation always improves the worst performing discrete frequency. This implies that the optimizer is using a lot of effort on the lowest specified frequency since that frequency will, at least at the start of the optimization, be the one with the largest individual value of the objective function. This means that the positive or negative outcome of the optimization is very much dependent on whether the optimizer is successful in raising the output at the lowest frequency. If the optimizer is unsuccessful in improving the lowest frequency the optimization will get stuck and the outcome is not a feasible solution. However, the min-max optimization formulation performs well when the lowest frequency can be improved as shown in this research, here we are able to create an almost flat response. An alternative formulation could be used in which the optimization problem would be an objective function summed over the frequency range of interest. In this case the optimizer will improve the frequencies where it is the most feasible. Such an optimization formulation will also make it possible to specify the frequency range lower than what has been done in this research, since we here at the start of the optimization are relying heavily on the optimizers ability to improve the lowest frequency.

The mass is by far the most influential parameter, since the stiffness of the surround of the passive radiator is sufficiently compliant. The two cases are therefor very close to being identical with regards

to performance in the frequency range of interest. It is seems to be advantageous for the optimizer to lower the stiffness further to decrease the resonance frequency without increasing the mass, this yields a softer roll-of and thereby a higher output at low frequencies. As the surround is becoming softer the stiffness of the air inside the cylinder starts to be important with regards to the resonance frequency of the passive radiator, lowering the stiffness of the surround is, as a consequence, becoming progressively less influential. However, we do show that by tuning the ratio of the stiffness of the surround to the stiffness of the air inside the cabinet of the speaker that we can enhance the low frequency performance of the passive radiator even further when compared to the mass tuned example.

5. CONCLUSION

The work presented utilizes gradient based multi-frequency optimization applied to a numerical model of a cylindrical loudspeaker. The optimization is used to tune the material properties of each individual component for a passive radiator such that the output at low frequencies are improved. We demonstrate the method for two examples. The mass tuned passive radiator where the density of the diaphragm is increased such that a feasible resonance peak is created and as a consequence the frequency range of the speaker unit is extended. The drawback of this method is that destructive interference is created immediately below the frequency range of interest. The second example shows that the optimal configuration of materials in a passive radiator is actually a lighter and less stiff diaphragm and surround when compared to the mass tuned example. This yields a flat response in the entire frequency range of interest which is almost an entire octave. Both examples increase the low frequency performance significantly.

The paper demonstrates the method and the benefits that can be gained from it at low frequencies, but the framework also allows for optimization at higher frequencies, which will be investigated in future work.

6. REFERENCES

[1] Edison Research and NPR, "The Smart Audio Report," tech. rep., 02 2020.

[2] H. F. Olson, "Loud speaker and method of propagating sound." U.S. Patent no. 1988250, application Feb. 1934, patented Jan. 1935.

[3] H. Olson, J. Preston, and E. May, "Recent developments in direct-radiator high-fidelity loudspeakers," *Audio Engineering Society – Journal*, vol. 2, no. 4, pp. 219–227, 1954.

[4] R. H. Small, "Passive-radiator loudspeaker systems .1. analysis," *Journal of the Audio Engineering Society*, vol. 22, no. 8, pp. 592–601, 1974.

[5] R. H. Small, "Direct-radiator loudspeaker system analysis," *IEEE Transactions on Audio and Electroacoustics*, vol. AU-19, no. 4, pp. 269–81, 269–281, 1971.

[6] G. H. Yoon, J. S. Jensen, and O. Sigmund, "Topology optimization of acoustic-structure interaction problems using a mixed finite element formulation," *International Journal for Numerical Methods in Engineering*, vol. 70, no. 9, pp. 1049–1075, 2007.

[7] J. S. Jensen, "A simple method for coupled acoustic-mechanical analysis with application to gradient-based topology optimization," *Structural and Multidisciplinary Optimization*, vol. 59, no. 5, pp. 1567–1580, 2019.

[8] E. Wadbro and M. Berggren, "Topology optimization of an acoustic horn," *Computer Methods in Applied Mechanics and Engineering*, 2006.

[9] C. S. Andreasen, M. O. Elingaard, and N. Aage, "Level set topology and shape optimization by density methods using cut elements with length scale control," *Structural and Multidisciplinary Optimization*, 2020.

[10] C. B. Dilgen, S. B. Dilgen, N. Aage, and J. S. Jensen, "Topology optimization of acoustic mechanical interaction problems: a comparative review," *Structural and Multidisciplinary Optimization*, vol. 60, no. 2, pp. 779–801, 2019.

[11] A. Bezzola, "Numerical optimization strategies for acoustic elements in loudspeaker design," *145th Audio Engineering Society International Convention, Aes 2018*, 2018.

[12] D. G. Nielsen, F. T. Agerkvist, and J. S. Jensen, "Optimization of realistic loudspeaker models with respect to basic response characteristics," *Proceedings of 23rd International Congress on Acoustics*, pp. 6219–6226, 2019.

[13] D. G. Nielsen, P. R. Andersen, J. S. Jensen, and F. T. Agerkvist, "Estimation of optimal values for lumped elements in a finite element -lumped parameter model of a loudspeaker," *Journal of Theoretical and Computational Acoustics*, to appear in 2020.

[14] J. N. Li, S. X. Wang, H. J. Yin, C. H. Dong, and H. M. Chen, "Acoustic wave equation modeling in cylindrical coordinates with convolutional pml," *77th Eage Conference and Exhibition 2015: Earth Science for Energy and Environment*, pp. 4546–4548, 2015.

[15] F. Collino and P. Monk, "The perfectly matched layer in curvilinear coordinates," *Siam Journal of Scientific Computing*, vol. 19, no. 6, pp. 2061–2090, 1998.

[16] J. S. Jensen, "Topology optimization problems for reflection and dissipation of elastic waves," *Journal of Sound and Vibration*, vol. 301, no. 1-2, pp. 319–340, 2007.

[17] K. Svanberg, "The method of moving asymptotes - a new method for structural optimization," *International Journal for Numerical Methods in Engineering*, 1987.